Non-uniform Mg distribution in GaN epilayers grown on mesa structures for applications in GaN power electronics

Cite as: Appl. Phys. Lett. **114**, 082102 (2019); https://doi.org/10.1063/1.5088168
Submitted: 08 January 2019 . Accepted: 14 February 2019 . Published Online: 26 February 2019

Hanxiao Liu, Houqiang Fu, Kai Fu, Shanthan R. Alugubelli, Po-Yi Su, Yuji Zhao, and Fernando A. Ponce

Applied Physics Letters ARTICLE scitation.org/journal/apl

Non-uniform Mg distribution in GaN epilayers grown on mesa structures for applications in GaN power electronics

Cite as: Appl. Phys. Lett. **114**, 082102 (2019); doi: 10.1063/1.5088168
Submitted: 8 January 2019 · Accepted: 14 February 2019 ·
Published Online: 26 February 2019

Hanxiao Liu,[1] Houqiang Fu,[2] Kai Fu,[2] Shanthan R. Alugubelli,[1] Po-Yi Su,[1] Yuji Zhao,[2] and Fernando A. Ponce[1,a)]

AFFILIATIONS

[1]Department of Physics, Arizona State University, Tempe, Arizona 85287, USA
[2]School of Electrical, Computer and Energy Engineering, Arizona State University, Tempe, Arizona 85287, USA

[a)]Email: ponce@asu.edu

ABSTRACT

A strong variation in the luminescence characteristics in Mg-doped GaN grown on mesa structures has been observed, with the sidewall luminescence being different from that of the flat regions. A comparison with the luminescence characteristics of Mg-doped GaN epilayers with different Mg concentrations indicates that the sidewall has a significantly lower Mg content. This observed non-uniform Mg distribution is attributed to the dependence of Mg incorporation efficiency on the crystal orientation of the growth surface, which should impact the electrical performance of power devices.

Gallium nitride (GaN) based power electronics has attracted much attention in recent years due to its advantages over traditional Si-based power devices in terms of energy conversion efficiency, switching frequency, operation temperature, and system volume.[1,2] Vertical architectures are usually preferred for high-voltage and high-power applications,[3–6] due to high voltage and current handling capability, good thermal management, and compact design. In the fabrication of advanced vertical power devices, such as normally-off vertical junction field effect transistors (VJFETs), junction barrier Schottky diodes, and superjunction diodes, it is important to produce laterally patterned *p-n* junctions and/or *p-uid* (unintentionally doped) junctions.

Selective-area doping using etch-and-regrowth procedures is one of the most effective ways to get controlled lateral junctions. Figure 1 shows the growth steps to produce the selective-area doped geometry used in this work. In this case, a film of *uid*-GaN or *n*-type GaN will be grown on a GaN substrate and then etched in certain areas to create a patterned mesa structure. A *p*-GaN layer will then be grown over the patterned mesa structures. Finally, the *p*-GaN on the upper mesa will be etched away to produce an alternating *p-uid* or *p–n* geometry.

During *p*-GaN regrowth, it is speculated that there could be two growth fronts, one on the basal plane in the upper and lower mesa flat regions and the other on inclined crystal planes at the mesa sidewall. This difference in growth orientation may result in varied Mg incorporation efficiency.[7–9] The Mg incorporation efficiency in these regions is a critical issue that can impact the performance of vertical power devices. For example, in VJFETs, the Mg doping level in *p*-GaN needs to be uniform and high enough to pinch off the channel without any bias, leading to a normally-off operation.[10] However, such variation in the Mg concentration cannot be characterized by secondary ion mass spectroscopy (SIMS), due to its lateral spatial resolution limitation. In this work, cathodoluminescence (CL) spectroscopy was used to investigate the optical properties of *p*-GaN in a mesa structure. A correlation among the Mg concentration, the optical properties, and the electronic properties of *p*-GaN has been established. This correlation has been used to extrapolate the Mg distribution in regrown *p*-GaN over a mesa structure at a sub-micron scale.

The epitaxial structures were grown by metal-organic chemical vapor deposition (MOCVD) on free-standing *c*-plane GaN substrates, with hydrogen as the carrier gas, at a growth temperature of 1050 °C. The Ga and N sources were trimethylgallium (TMGa) and ammonia (NH_3), respectively. The precursor for Si donors was silane (SiH_4), and the precursor for Mg acceptors is bis(cyclopentadienyl)magnesium (Cp_2Mg). More details on the MOCVD growth can be found elsewhere.[11,12] We report on the properties of four thin film structures, labeled A to D. The initial layer of sample A consists of 4 μm of *uid*-GaN grown on the *c*-plane GaN substrate. The *uid*-GaN layer was

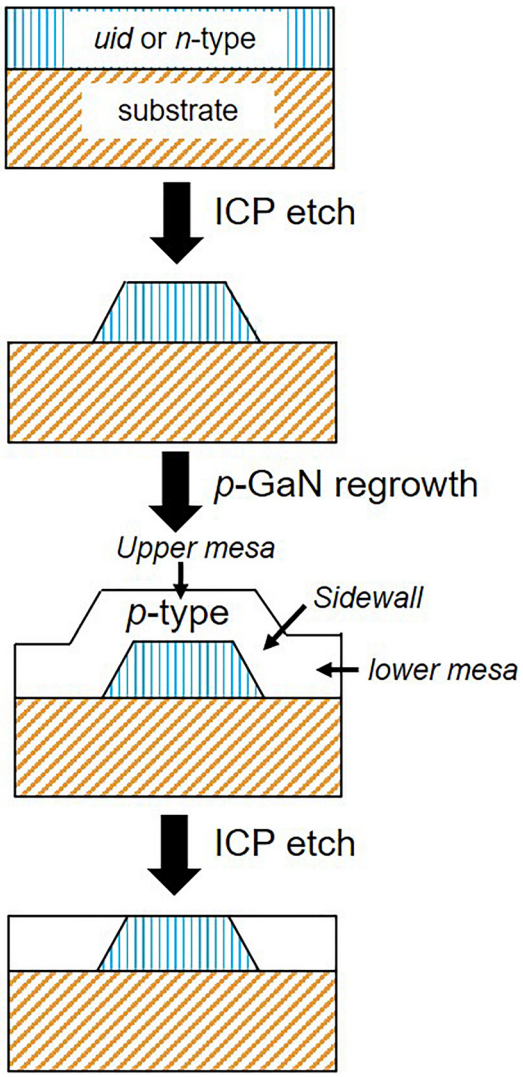

FIG. 1. Growth sequence to produce a selective-area doped geometry in GaN, using the etch-and-regrowth procedure used in this work.

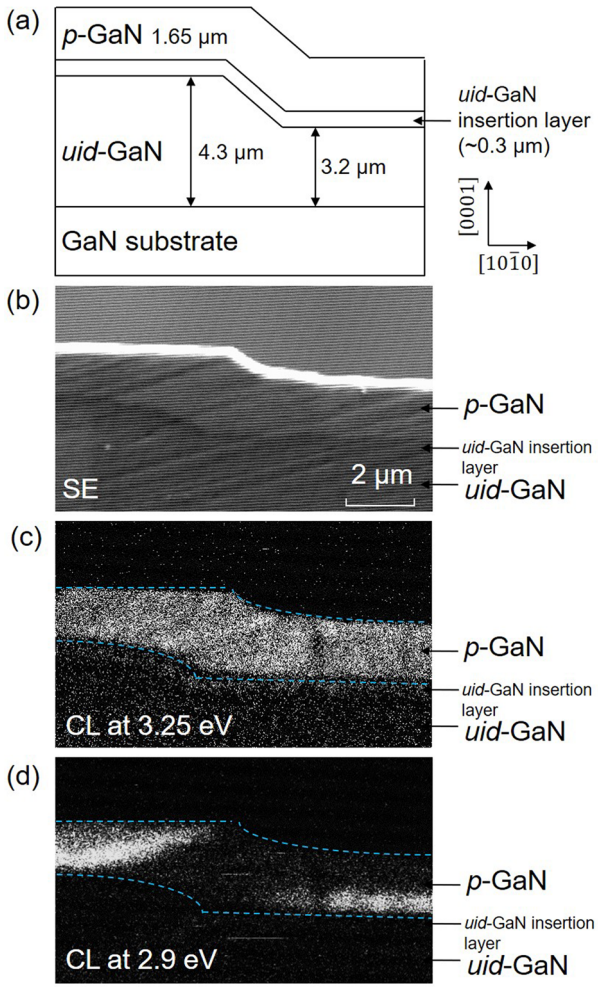

FIG. 2. Cross-sectional view of the *p*-GaN/*uid*-GaN mesa structure in sample A. (a) Schematic drawing of the thin film structure, with the sidewall along *a*-directions ($\langle 11\bar{2}0\rangle$). (b) SE image using a 7 kV primary beam. Monochromatic CL images at (c) 3.25 eV and (d) 2.9 eV. The dashed lines follow the differently doped homojunctions, as determined from (c).

then selectively etched to produce periodic mesa structures. Etching was done by photolithography and chlorine-based inductively coupled plasma (ICP) dry etching (at an ICP/RF power of 400/70 W, a Cl_2/BCl_3/Ar flow rate of 30/8/5 sccm, and a pressure of 0.67 Pa). Following the etching, 0.3 μm of *uid*-GaN and 1.65 μm of the *p*-GaN film were grown over the mesa structures. The *p*-GaN was grown with a TMGa flow rate of 25 sccm and a Cp_2Mg flow rate of 100 sccm, at a temperature of 950 °C. The schematic drawing of one of the mesa structures is shown in Fig. 2(a). Another series of samples (samples B–D) were grown to investigate the effect of the Cp_2Mg flow rate on the *p*-GaN optical and electronic properties. Their structure consists of 1 μm *p*-GaN on 2 μm *n*-GaN grown on sapphire substrates. The growth conditions of these 3 samples were identical, except that three different Cp_2Mg flow rates of 50, 100, or 200 sccm were used during the growth of the *p*-GaN film to achieve different Mg doping concentrations.

Post-growth thermal activation of *p*-GaN was performed on all samples using rapid thermal annealing at 800 °C for 10 min in a nitrogen atmosphere. The Mg concentrations in the *p*-GaN layer of samples B–D were determined by secondary ion mass spectroscopy (SIMS). Hole concentrations and hole mobility of the *p*-GaN films in samples B–D were measured at room temperature with the Hall effect using the van der Pauw method. The optical properties of all samples were studied using cathodoluminescence (CL) spectroscopy. The CL system consists of a JEOL 6300 scanning electron microscope (SEM) connected to an Oxford CL2 monochromator and a photomultiplier tube. Spot mode CL spectra were obtained by fixing the electron beam at a specific location on the sample and scanning the spectrum across the desired wavelength range. CL mappings were obtained by setting the monochromator to a certain wavelength and recording the spatial variation of luminescence intensity over an area. The electron beam

current used in our CL studies was 100 pA, with an acceleration voltage of 7 kV.

The optical properties of sample A, with the mesa structure, were studied in cross-section by CL imaging and spectroscopy. The cross-sectional samples were prepared by mechanical polishing. Figure 2(a) shows a schematic diagram of the cross-sectional view of one of the mesa steps. Figures 2(b) is a secondary electron (SE) image; (c) and (d) are CL mappings at 3.25 and 2.9 eV, respectively. A mesa step with 1.1 μm in height, resulting from the ICP etching, is observed in the SE image. The mesa has a hexagonal shape with the sides along a-directions ($\langle 11\bar{2}0 \rangle$), as indicated in Fig. 2(a). The sidewall initially makes approximately a 28° angle with respect to the basal plane, which corresponds to a $\{1\bar{1}02\}$ plane, and then approaches the basal plane. A *p*-GaN layer with a thickness of 1.65 μm was grown above the mesa structure. The CL mapping at 3.25 eV in Fig. 2(c) shows that the *p*-GaN layer exhibits a uniform emission at that energy. The CL mapping at 2.9 eV in Fig. 2(d), however, shows a lower emission in the vicinity of the sidewall. Figure 3(a) is also a CL mapping at 2.9 eV but at a lower magnification compared to Fig. 2(d). It is observed that the lower mesa, adjacent to the sidewall, also exhibits a weak emission intensity at 2.9 eV. However, the area of the low intensity portion in the lower mesa gradually recedes as the distance from the sidewall increases. When sufficiently far away (>10 μm) from the sidewall, the lower mesa has a uniform and strong emission at 2.9 eV, similar to that in the upper mesa. It should be noted that such a non-uniform luminescence pattern is repeatedly observed near all the mesa steps.

Spot mode CL spectra were taken at five different locations within the *p*-GaN layer, as indicated in Fig. 3(a): upper mesa, sidewall, top of the lower mesa, bottom of the lower mesa, and center of the lower mesa away from the sidewall. The interaction volume of the electron beam is estimated to be around 400 nm in diameter, which is smaller than the *p*-GaN layer thickness of 1.65 μm. Therefore, the CL signal should only originate from the *p*-GaN layer. The spot mode CL spectra are plotted in Fig. 3(b). Three common peaks at 3.4, 3.25, and 2.9 eV are observed at all locations. The spectral shape is similar for the upper mesa, bottom of the lower mesa, and the center of the lower mesa away from the sidewall, where emission is dominated by the 2.9 eV peak. The emissions at the sidewall and the top of the lower mesa are dominated by the 3.4 and 3.25 eV peaks, while the 2.9 eV peak is very weak, as has been visualized in the CL mapping in Fig. 3(a).

In order to establish a correlation between the doping concentration and the optical and electronic properties of *p*-GaN films, we have studied samples B–D, which have an epilayer structure of 1-μm *p*-GaN on 2-μm *n*-GaN on sapphire, a schematic diagram of which is shown in the inset of Fig. 4. The Cp_2Mg flow rates used for *p*-GaN growth were 50 sccm, 100 sccm, and 200 sccm, for samples B–D, with the corresponding Mg concentrations as determined by SIMS to be 1.3×10^{19}, 3.1×10^{19}, and 6.3×10^{19} cm^{-3}, respectively. The CL spectra in Fig. 4 show three peaks at 3.4, 3.25, and 2.9 eV. The relative intensity of the 2.9 eV peak as compared to the 3.25 eV peak increases with the Mg concentration in the film.

Hole concentrations and mobilities of the *p*-GaN layer in samples B–D are summarized in Table I. Sample B is resistive with no reliable Hall effect reading available. Sample C with [Mg] = 3.1×10^{19} cm^{-3} presents a hole concentration of 1.3×10^{17} cm^{-3} and a mobility of 9.5 cm^2/(V s). Sample D with [Mg] = 6.3×10^{19} cm^{-3} has a hole concentration of 2×10^{17} cm^{-3} and a mobility of 6.0 cm^2/(V s).

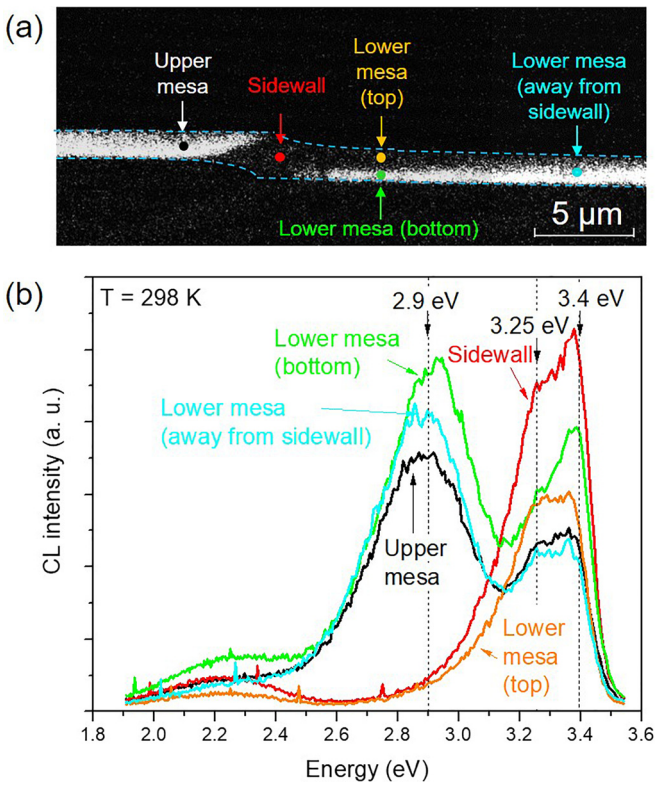

FIG. 3. Cross-sectional optical properties of the *p*-GaN/*uid*-GaN mesa structure in sample A. (a) Monochromatic CL mapping at 2.9 eV. (b) Spot-mode CL spectra in different regions in the *p*-GaN layer as indicated by arrows in (a).

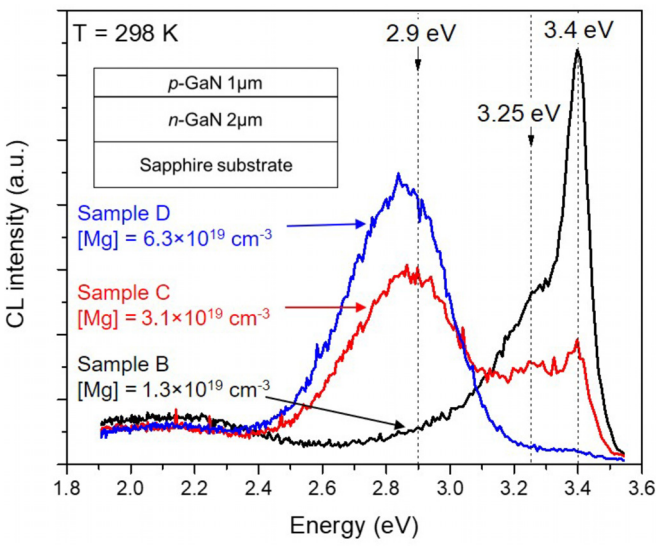

FIG. 4. CL spectra of *p*-GaN layers with different Mg concentrations (samples B–D). A schematic drawing of the sample structure of samples B–D is shown in the inset.

TABLE I. Summary of the Mg concentration ([Mg]), hole concentration ([h]), and hole mobility of *p*-GaN layers with different Mg concentrations (samples B–D).

	[Mg]	[h]	Hole mobility
Sample B	1.3×10^{19} cm^{-3}	Too resistive	Too resistive
Sample C	3.1×10^{19} cm^{-3}	1.3×10^{17} cm^{-3}	9.5 cm^2/(V s)
Sample D	6.3×10^{19} cm^{-3}	2.0×10^{17} cm^{-3}	6.0 cm^2/(V s)

The transitions observed in the CL spectra have been previously reported for Mg-doped GaN.[13–16] The 3.4 eV peak has been attributed to near-band-edge excitonic transitions at room temperature, the 3.25 eV peak to shallow-donor to Mg-acceptor transitions, and the 2.9 eV peak to deep-donor to Mg-acceptor transitions. The origin of deep donor states is of much debate, but the commonly accepted view is that they are complexes formed by nitrogen vacancies with the nearest neighbor Mg atoms (V_N-Mg_{Ga}).[14–16] The relative intensities of these peaks change with [Mg], as shown in Fig. 4. When [Mg] is increased, the intensities of the high-energy peaks (3.4 eV and 3.25 eV) decrease and the intensity of the low energy peak (2.9 eV) increases.[13,14,16]

To explain the change in the light emission characteristics of *p*-GaN with increasing Mg concentrations, we propose a model, depicted in Fig. 5. The shallow and deep donor states are initially neutral (occupied by electrons). They are ionized by transferring electrons to the acceptors (self-compensation) or thermally exciting electrons to the conduction band. When the shallow or deep donors are ionized, their states are available for radiative recombination and can contribute to light emission at 3.25 or 2.9 eV, respectively. For *p*-GaN with low [Mg] in Fig. 5(a), there are not enough acceptors to accept the electrons from both shallow and deep donors. In this case, only part of the shallow donors is ionized, and the deep donors are neutral. Therefore, light emission will originate from band edge transitions (3.4 eV) and shallow donor to acceptor transitions (3.25 eV), as observed in Fig. 4 for sample B with [Mg] $= 1.3 \times 10^{19}$ cm^{-3}. For *p*-GaN with high [Mg] in Fig. 5(b), there are sufficient acceptor states to accept electrons from both shallow and deep donors, leading to complete ionization (unoccupied electron states). An electron excited to the conduction band in this sample will relax to the lowest energy state (deep donor state) and then via a radiative transition to the acceptor states causing luminescence at 2.9 eV, as observed in Fig. 4 for sample D with [Mg] $= 6.3 \times 10^{19}$ cm^{-3}. At medium [Mg], deep donor states are partially ionized, and optical transition happens at 2.9 eV. Depending on the excitation power, some electrons will also recombine from shallow-donor states or from the conduction band edge, producing 3.25 eV and 3.4 eV emissions, as in Fig. 4, for sample C with [Mg] $= 3.1 \times 10^{19}$ cm^{-3}.

We use spot mode CL to probe local variations of [Mg] in the *p*-GaN films with sub-micron resolution. By comparing the CL spectra taken at various locations of the mesa structure [Fig. 3(b)] to the CL spectra of *p*-GaN with different [Mg] (Fig. 4), we can see some similarities. The spectra from the upper mesa, bottom of the lower mesa, and the center of the lower mesa away from the sidewall in Fig. 3(b) closely resemble the spectrum of sample C with [Mg] $= 3.1 \times 10^{19}$ cm^{-3} in Fig. 4. This is expected, because the *p*-GaN layer growth conditions in these two samples (samples A and C) are identical with the same Cp_2Mg flow rate of 100 sccm. On the other hand, the spectra from the sidewall and the top of the lower mesa closely resemble the spectrum of sample B with [Mg] $= 1.3 \times 10^{19}$ cm^{-3} in Fig. 4. This implies that [Mg] in the sidewall and top of the lower mesa are lower.

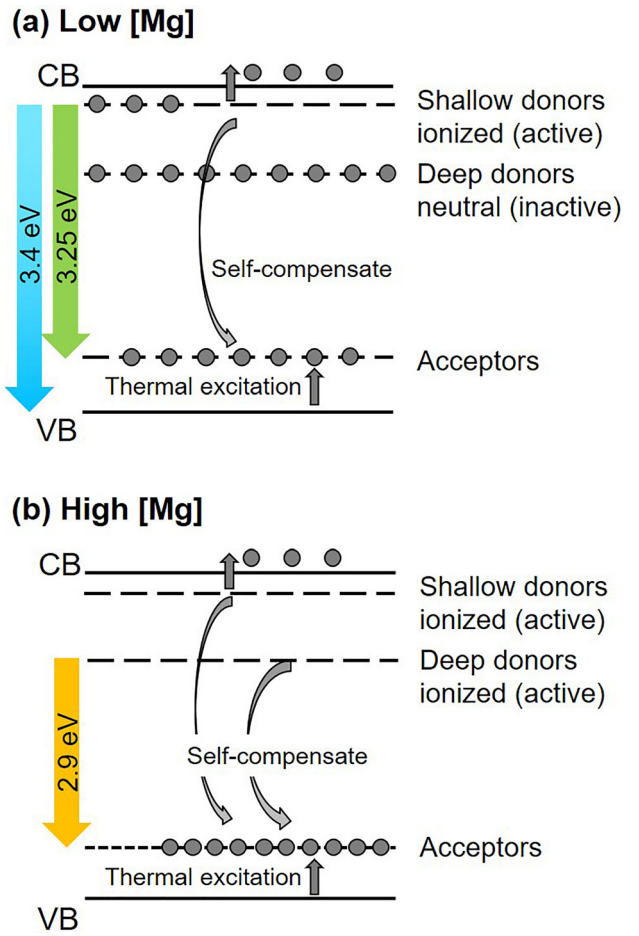

FIG. 5. Illustration to explain the different luminescence characteristics of *p*-GaN with (a) low and (b) high magnesium concentrations.

We attribute the non-uniform Mg concentration in the mesa structure to Mg incorporation efficiency during growth on different crystal planes. The bright and dark regions in *p*-GaN in Fig. 3(a) represent higher and lower Mg contents, respectively. This is due to the vertical growth (perpendicular to the basal plane) at the flat surfaces in the upper and lower sections of the mesa and growth on inclined crystal planes near the sidewall. This finding suggests that CL spectroscopy can also be utilized as a tool to visualize the growth front of Mg-doped GaN on uneven structures.

In conclusion, selective area doping of Mg in GaN has been achieved by etch-and-regrowth processes. Spot mode CL spectroscopy and CL mapping have been used to reveal that the sidewall of Mg-doped GaN grown over a mesa structure is Mg deficient. The lower Mg concentration at the sidewall is attributed to inefficient Mg incorporation at non-basal crystal planes. CL mapping was used to illustrate the growth mechanism in a mesa structure where vertical growth and tilted growth take place simultaneously in close vicinity.

This work was supported by the ARPA-E PNDIODES Program monitored by Dr. Isik Kizilyalli. We acknowledge the use of facilities within the Eyring Materials Center at Arizona State University. The device fabrication was performed at the Center for Solid State Electronics Research at Arizona State University. Access to the NanoFab was supported, in part, by NSF Contract No. ECCS-1542160.

REFERENCES

[1]S. Chowdhury and U. K. Mishra, IEEE Trans. Electron Devices **60**, 3060 (2013).
[2]U. K. Mishra, L. Shen, T. E. Kazior, and Y.-F. Wu, Proc. IEEE **96**, 287 (2008).
[3]I. C. Kizilyalli, A. P. Edwards, O. Aktas, T. Prunty, and D. Bour, IEEE Trans. Electron Devices **62**, 414 (2015).
[4]I. C. Kizilyalli, A. P. Edwards, H. Nie, D. Disney, and D. Bour, IEEE Trans. Electron Devices **60**, 3067 (2013).
[5]H. Fu, X. Huang, H. Chen, Z. Lu, I. Baranowski, and Y. Zhao, Appl. Phys. Lett. **111**, 152102 (2017).
[6]M. Sun, Y. Zhang, X. Gao, and T. Palacios, IEEE Electron Device Lett. **38**, 509 (2017).
[7]S. C. Cruz, S. Keller, T. E. Mates, U. K. Mishra, and S. P. DenBaars, J. Cryst. Growth **311**, 3817 (2009).
[8]A. Chakraborty, H. Xing, M. D. Craven, S. Keller, T. Mates, J. S. Speck, S. P. DenBaars, and U. K. Mishra, J. Appl. Phys. **96**, 4494 (2004).
[9]J. Wang, Y. Gao, S. Alam, and F. Scholz, Phys. Status Solidi A **211**, 2645 (2014).
[10]D. Ji and S. Chowdhury, IEEE Trans. Electron Devices **62**, 2571 (2015).
[11]S. Nakamura, G. Fasol, and S. J. Pearton, *The Blue Laser Diode: The Complete Story*, 2nd ed. (Springer, Heidelberg, 2000).
[12]Y. Zhao, H. Fu, G. T. Wang, and S. Nakamura, Adv. Opt. Photonics **10**, 246 (2018).
[13]H. Amano, M. Kitoh, K. Hiramatsu, and I. Akasaki, J. Electrochem. Soc. **137**, 1639 (1990).
[14]U. Kaufmann, M. Kunzer, M. Maier, H. Obloh, A. Ramakrishnan, B. Santic, and P. Schlotter, Appl. Phys. Lett. **72**, 1326 (1998).
[15]F. Shahedipour and B. W. Wessels, Appl. Phys. Lett. **76**, 3011 (2000).
[16]H. Obloh, K. H. Bachem, U. Kaufmann, M. Kunzer, M. Maier, A. Ramakrishnan, and P. Schlotter, J. Cryst. Growth **195**, 270 (1998).